

RESEARCH ARTICLE

10.1002/2015WR018023

Key Points:

- Macroscale behavior of sediment transport reveals aspects of microscale particle dynamics
- Heavy-tailed particle resting times can result in both sub and superdiffusion
- Higher-order statistical moments are needed to differentiate between various complexity models

Correspondence to:

N. Fan,
fannian7172@126.com

Citation:

Fan, N., A. Singh, M. Guala, E. Fofoula-Georgiou, and B. Wu (2016), Exploring a semimechanistic episodic Langevin model for bed load transport: Emergence of normal and anomalous advection and diffusion regimes, *Water Resour. Res.*, 52, 2789–2801, doi:10.1002/2015WR018023.

Received 27 AUG 2015

Accepted 9 MAR 2016

Accepted article online 14 MAR 2016

Published online 9 APR 2016

Exploring a semimechanistic episodic Langevin model for bed load transport: Emergence of normal and anomalous advection and diffusion regimes

Niannian Fan^{1,2,3}, Arvind Singh⁴, Michele Guala³, Efi Foufoula-Georgiou³, and Baosheng Wu²

¹State Key Laboratory of Hydraulics and Mountain River Engineering, College of Water Resource and Hydropower, Sichuan University, Chengdu, Sichuan, China, ²State Key Laboratory of Hydrosience and Hydraulic Engineering, Tsinghua University, Beijing, China, ³Department of Civil, Environmental and Geo-Engineering, Saint Anthony Falls Laboratory and National Center for Earth-Surface Dynamics, University of Minnesota, Minneapolis, Minnesota, USA, ⁴Department of Civil, Environmental, and Construction Engineering, University of Central Florida, Orlando, Florida, USA

Abstract Bed load transport is a highly stochastic, multiscale process, where particle advection and diffusion regimes are governed by the dynamics of each sediment grain during its motion and resting states. Having a quantitative understanding of the macroscale behavior emerging from the microscale interactions is important for proper model selection in the absence of individual grain-scale observations. Here we develop a semimechanistic sediment transport model based on individual particle dynamics, which incorporates the episodic movement (steps separated by rests) of sediment particles and study their macroscale behavior. By incorporating different types of probability distribution functions (PDFs) of particle resting times T_r , under the assumption of thin-tailed PDF of particle velocities, we study the emergent behavior of particle advection and diffusion regimes across a wide range of spatial and temporal scales. For exponential PDFs of resting times T_r , we observe normal advection and diffusion at long time scales. For a power-law PDF of resting times (i.e., $f(T_r) \sim T_r^{-\nu}$), the tail thickness parameter ν is observed to affect the advection regimes (both sub and normal advective), and the diffusion regimes (both subdiffusive and superdiffusive). By comparing our semimechanistic model with two random walk models in the literature, we further suggest that in order to reproduce accurately the emerging diffusive regimes, the resting time model has to be coupled with a particle motion model able to produce finite particle velocities during steps, as the episodic model discussed here.

1. Introduction

The nature of bed load transport is highly stochastic and complex, even under steady state conditions, involving a wide range of spatiotemporal scales, from grain-scale kinematics to bed form-scale migration [Sekine and Parker, 1992; Papanicolaou et al., 1999; Ancy et al., 2006; Ancy, 2010; Hill et al., 2010; Singh et al., 2009, 2011, 2012; Ramesh et al., 2011; Furbish et al., 2012a; McElroy and Mohrig, 2012; Julien and Bounvilay 2013; Guala et al., 2014; Keylock et al., 2014; Cristo et al., 2015]. This inherent stochasticity is mostly a result of the particle-fluid interactions and particle-particle interactions, leading to diffusion (also referred to as dispersion) of particles during their movement [Martin et al., 2012].

Particle diffusion, based on individual tracing particles, has been studied by several researchers [e.g., see Sayre and Hubbell, 1965; Yang and Sayre, 1971; Todorovic, 1982; Drake et al., 1988; Ferguson and Wathen, 1998 for some early studies]. However, following the seminal work of Nikora et al. [2001, 2002], studies of anomalous diffusion have recently blossomed from flume experiments [e.g., Martin et al., 2012; Ballio et al., 2013; Campagnol et al., 2015], field investigations [e.g., Hassan et al., 2013; Phillips et al., 2013; Haschenburger, 2013], and numerical simulations [e.g., Bradley et al., 2010; Bialik et al., 2012; Zhang et al., 2012, 2014; Pelosi et al., 2014].

While field investigation in natural rivers can provide large-scale characteristics of sediment motions, it faces limitation in revealing particle-scale dynamics [Hassan et al., 1991, 2013; Haschenburger, 2013]. On the contrary, flume experiments, especially with the deployment of new optically based observational techniques, could reveal detailed information at the particle scale, but face difficulty in capturing particle transport

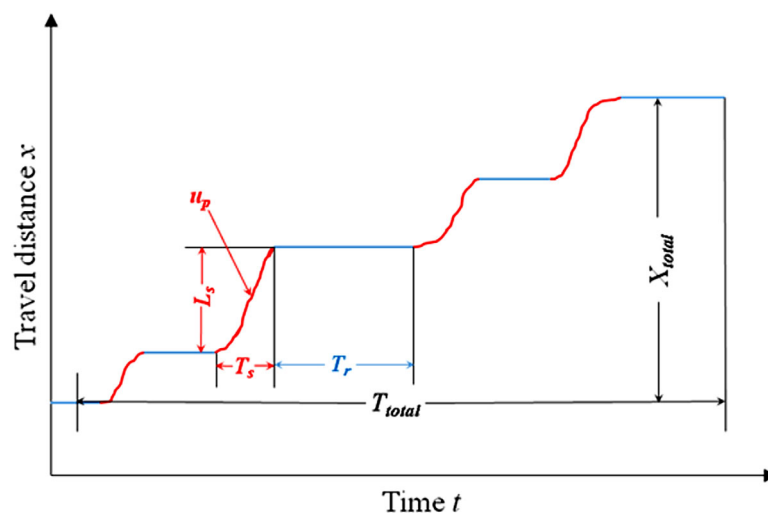


Figure 1. Schematic for the episodic motion of one particle. Steps are separated by rests, moving and resting states are represented by red and blue lines, respectively. The step lengths L_s , step times T_s , velocities of moving particle u_p , and the resting times T_r are all stochastic variables.

characteristics across a large enough spatial and temporal range of scales, e.g., due to the limitation of the sampling size window [Furbish *et al.*, 2012a; Martin *et al.*, 2012; Campagnol *et al.*, 2015]. As a result, simulating particle trajectories by employing physically informed models, calibrated on experimental data, could be a promising avenue to study the emergent macroscale behavior of particle advection and diffusion.

Bed load particles move episodically, through discrete steps separated by rests, as depicted in Figure 1, suggesting that step lengths L_s (also referred to as jump lengths or hop distances), step times T_s , resting times T_r (also referred to as waiting times or residence times), and velocities of active particles u_p , can be all treated as stochastic variables. It has been suggested that, if the probability density functions (PDFs) of these variables, namely, u_p , L_s , T_s , and T_r are all thin tailed, the resulting particle diffusion regime is always normal for all scales [Han and He, 1980], except for superdiffusion (ballistic) at very short initial time scales due to particles' inertia [Nikora *et al.*, 2002]. In contrast, anomalous diffusion (super or subdiffusion) can result from the heavy-tailed PDFs of, at least one, of those variables (u_p , L_s , T_s , and T_r). Both Schumer *et al.* [2009] and Weeks *et al.* [1996] used a random walk models (RWM) to simulate the episodic motion of particles, combining discrete steps separated by rests. They also illustrated how normal or anomalous diffusion could result from different types of PDFs of step lengths L_s and resting times T_r , based on the PDF-tail thickness. However, the Schumer *et al.* [2009] model (hereafter referred to as S-RWM) and the Weeks *et al.* [1996] model (hereafter referred to as W-ARWM, "A" refers to asymmetric) predict different diffusion regimes under similar initial conditions. It is still an open question of great interest to study how the diffusion regime is controlled by the (joint) distributions of u_p , L_s , T_s , and T_r [Martin *et al.*, 2012; Hassan *et al.*, 2013], potentially including also the effect of particle-size heterogeneity [Ganti *et al.*, 2010; Hill *et al.*, 2010].

For bed load particles, several studies considered the PDF of step lengths L_s as thin tailed, including the exponential distribution [e.g., Einstein, 1937; Sayre and Hubbell, 1965; Schmidt and Ergenzinger, 1992; Habersack, 2001; Wu and Yang, 2004] or the gamma distribution [e.g., Yang and Sayre, 1971; Lajeunesse *et al.*, 2010], whereas Bradley *et al.* [2010] treated it as a heavy-tailed distribution. Generally, the number of step lengths L_s extracted from experiments is often relatively small, preventing a robust analysis on the tails of the distribution [Martin *et al.*, 2014]; besides, large step lengths L_s might also be missed due to limitations in the sample size window [Phillips *et al.*, 2013], implying that the tails of the PDFs of L_s from the previous studies might not be so clear to interpret. Similar to step lengths L_s , the PDFs of resting times T_r have not been consistently quantified by several studies [see Zhang *et al.*, 2014 for a review]. For example, both exponential distributions [Einstein, 1937; Yang and Sayre, 1971; Schmidt and Ergenzinger, 1992; Habersack, 2001; Wu and Yang, 2004; Valyrakis *et al.*, 2011; Furbish *et al.*, 2012b], and heavy-tailed distributions (power-law, Martin *et al.* [2012; 2014] or tempered Pareto, Voepel *et al.* [2013]) were observed.

Despite the ambiguities in the PDFs of both step lengths L_s and resting times T_r , the tail of the PDF of active particle velocities u_p has been observed to be thin tailed by several studies, e.g., exponential distribution by Roseberry *et al.* [2012], Furbish *et al.* [2012c], Furbish and Schmeeckle [2013], Fathel *et al.* [2015], or Gaussian distribution by Ancey and Heyman [2014] and Martin *et al.* [2012].

Both the models by Fan *et al.* [2014] and Ancey and Heyman [2014], developed and calibrated on experimental data, are based on the Langevin equation which describes the forces exerted on a single particle. In particular, the Fan *et al.* [2014] model was developed for uniform particles under low bed load transport conditions and was calibrated using the experimental data by Roseberry *et al.* [2012]. The evolution of individual particle velocities u_p was expressed as a function of the actual forces acting on the particle, incorporating both a deterministic and a stochastic component. By simulating many particle trajectories, the Fan *et al.* [2014] model was able to reproduce both the thin tailed probability density function (PDF) of the moving particle velocities (a typical collective or macro-scale quantity) and the relationship between step times T_s and the associated step lengths L_s (representative of grain-scale kinematics). However, the particles simulated by the model of Fan *et al.* [2014] were always assumed to be in motion. Here, we extend the Fan *et al.* [2014] model to include particle resting, by incorporating a resting time stochastic model leading to an Episodic Langevin Equation (ELE) able to reproduce the more realistic particle episodic behavior at low transport rates.

We acknowledge that our model may not be able to rigorously predict the transport process of tracer particles, because the resting time model has not been validated on experimental data. However, the simulation results can help us to better understand how the emergent advection and diffusion regimes, i.e., the first and second-order moments of travel distances, respectively, are constrained by the particles' motion and resting time statistical characteristics. In particular, we want to understand if and how different tails of the statistical distribution of the resting time T_r can be a source of anomalous diffusion.

The paper is structured as follows. In section 2, we introduce the episodic formulation of the Langevin Equation (ELE), to simulate the tracer particle switching between active and resting regimes. In sections 3 and 4, we study the transport of uniform particles, testing exponential PDFs and power-law PDFs of resting times T_r , respectively. In section 5, we compare the advection and diffusion regimes obtained using our ELE model to those resulting from the Langevin equation proposed by Ancey and Heyman [2014] extended to incorporate episodic movement. In section 6, we compare the three models (Schumer *et al.* [2009] S-RWM, Weeks *et al.* [1996] W-ARWM, and our ELE) and discuss the emergence of their diffusion regimes. Conclusions are presented in section 7.

2. Episodic Particle Transport Framework

Fan *et al.* [2014] proposed a Langevin equation (LE) to describe the temporal evolution of a particle velocity based on the forces exerted on it. In the streamwise direction, for a single particle per unit mass, the LE was expressed as follows:

$$\frac{du_p}{dt} = -\Delta_x \cdot \text{sign}(u_p) + F_x + \zeta_x \quad (1)$$

where t is time, u_p is the streamwise velocity, Δ_x is a constant for Coulomb-like friction force; F_x is an average downstream force (including drag and gravity), and ζ_x is a fluctuating, stochastic force. A stochastic Runge-Kutta numerical algorithm was used to discretize the LE as

$$\begin{aligned} F_1 &= -\Delta_x \cdot \text{sign}[u_p(t) + w_1 \sqrt{2D_x \Delta t}] + F_x \\ F_2 &= -\Delta_x \cdot \text{sign}[u_p(t) + \Delta t \cdot F_1 + w_2 \sqrt{2D_x \Delta t}] + F_x \\ u_p(t + \Delta t) &= u_p(t) + \frac{1}{2}(F_1 + F_2)\Delta t + w_0 \sqrt{2D_x \Delta t} \end{aligned} \quad (2)$$

where F_1 and F_2 are the Runge-Kutta coefficients; w_0 , w_1 , and w_2 are independent Gaussian random variables with zero mean and unit variance; and D_x denotes the magnitude of a fluctuating, stochastic force (see Fan *et al.* [2014] for more details about the LE model, and for its calibration based on the experimental data by Roseberry *et al.* [2012]).

While the LE model (equation (1)) provides an adequate description for particles in motion, it does not incorporate the possibility of episodic particle resting on the bed. In real systems, however, the particle velocity fluctuates significantly and may often fall to zero, leading to the particle stopping for a while and continuously switching between resting and moving regimes. Here we extend the LE to incorporate a resting time in an episodic framework resulting in an Episodic Langevin Equation (ELE) which can mimic more realistically the nature of episodic particle motion. The ELE framework can be expressed as follows:

1. We use equation (2) to simulate a single particle velocity series (active particle motion regime);
2. We impose the particle velocity to be zero when its velocity turns from positive to negative (or from negative to positive), forcing the particle to stop (the velocity remains zero) for a duration defined by the stochastic resting time T_r (particle resting regime);
3. After T_r , the particle is allowed to move again, according to equation (2).

We acknowledge that the criterion as noted in (2) for particle deposition is only a working assumption. It is indeed possible that a particle bounding on the river bed may reverse its velocity before and after the contact such that, at some point in time, it reaches zero velocity without necessarily stopping. However, for low bed load transport rates, as those simulated here and measured by *Roseberry et al.* [2012], it seems a reasonable assumption. In the simulations below, we keep the same values of parameters used in *Fan et al.* [2014] ($\Delta_x = 3.66 \text{ m} \cdot \text{s}^{-2}$, $F_x = 3.17 \text{ m} \cdot \text{s}^{-2}$, and $D_x = 0.0223 \text{ m}^2 \cdot \text{s}^{-3}$) to model the motion regime in the ELE, but we increased the simulation time step to $\Delta t = 10^{-3} \text{ s}$ in order to accommodate much longer trajectories. Figure 2a shows a realization of a simulated velocity time series for one particle depicting the episodic characteristic of particle movement. The travel distance x during a certain time t may consist of several steps, while the total time t consists of a sequence of step and resting times. Note that for both $\Delta t = 10^{-3} \text{ s}$, in this paper, and $\Delta t = 10^{-4} \text{ s}$, in *Fan et al.* [2014], the velocities of the active particles (abandoning zero velocities) maintain the same thin-tailed, exponential-like PDF derived by the LE of *Fan et al.* [2014] (not presented here for brevity). Figure 2b shows the simulated step times T_s versus step lengths L_s , suggesting a power-law $L_s \propto T_s^{1.6}$ relationship. The exponent 1.6 is very close to 5/3, also obtained from the experimental data by *Roseberry et al.* [2012]. This result is obtained from 16,903 steps, extracted from 100 simulated particles moving simultaneously for a duration of 40 s, with a minimum resting time T_r set to 0.001 s (equal to the simulation time step Δt), and excluding step lengths less than 0.005 cm. In our simulation, the step lengths L_s , step times T_s , and the velocities u_p of the moving particle are embedded in the particle motion model (explicitly related to the model parameters Δ_x , F_x , and D_x) while the resting times T_r are provided by an independent model capable to explore different statistical distributions of T_r .

3. ELE With Exponential PDF of Resting Times

Using the ELE model discussed in section 2, we simulated the motion of a large number of uniform size particles with exponential PDF of resting times T_r . The ratio of average resting time over average step time \bar{T}_r / \bar{T}_s was set to different values, namely 5, 25, and 125, representing different transport rates.

Particles in a continuous motion regime ($T_r = 0$) are also simulated for comparison. We acknowledge that we keep the set of parameters (Δ_x , F_x , and D_x) invariant for different ratios of \bar{T}_r / \bar{T}_s . To change these parameters, we would need experimental data under different transport regimes which are not available. From the simulated data, we study the characteristics of the resulting advection and diffusion regimes after the particle release ($x=0$, $t=0$). In the initial conditions ($t=0$): (a) the model has been “warmed up” to achieve the steady PDF (exponential-like) of the moving particles velocities; (b) all the particles are in the same position $x=0$ (without accounting for particle-particle interactions or collisions, in a mechanistic way). All the following simulations use the same initial conditions described here.

3.1. Particle Advection

The advection process governs how quickly particles are transported downstream: it can be quantified by the growth of the mean particle travel distances x with time t

$$\langle x \rangle \propto t^{\alpha_x}. \tag{3}$$

Here $\langle x \rangle$ represents the ensemble average of every travel distance x_i for every individual particle, whereas α_x represents the scaling exponent. When $\alpha_x = 1$, particle advection is “normal,” i.e., the mean grows linearly

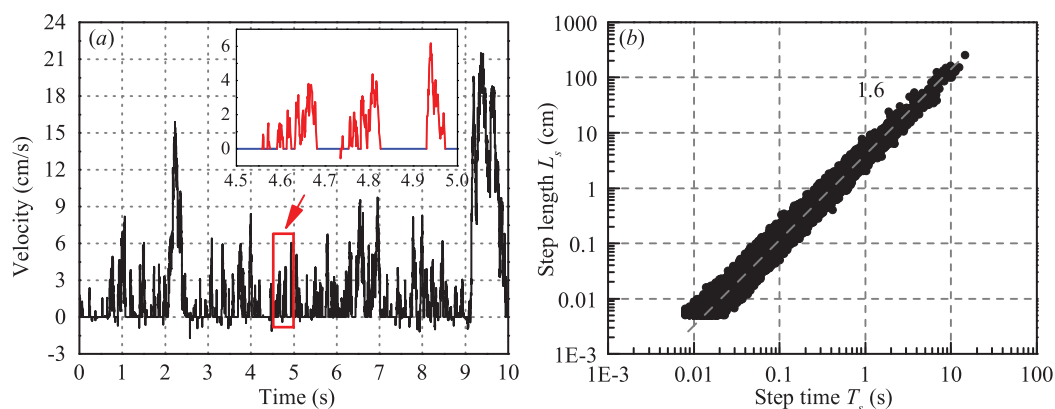


Figure 2. Simulated particles using the Episodic-Langevin-Equation (ELE). (a) A simulated velocity time series for a single particle obtained from the ELE for a duration of 10 s. Inset plot shows a zoomed-in time series for a duration of 0.5 s. Note the episodic behavior of the particle, i.e., stopping and moving (in the inset plot) represented by the blue and red lines, respectively. (b) Simulated step times T_s versus step lengths L_s suggesting a power-law $L_s \propto T_s^{1.6}$ relationship. The exponent 1.6 is very close to 5/3, also obtained from the experimental data by Roseberry *et al.* [2012].

with time. When $\alpha_x \neq 1$, particle advection is “anomalous,” specifically, subadvection for $\alpha_x < 1$ and superadvection for $\alpha_x > 1$ [Weeks and Swinney, 1998].

Figure 3a represents particle advection for different \bar{T}_r/\bar{T}_s ratios, all showing normal advection ($\alpha_x=1$) for the entire range of time scales investigated here. Note that here time t is normalized by d/u_* (see also Nikora *et al.* [2002]), where d is the particle diameter and u_* is the friction velocity (assumed to be 0.5 mm and 2.01 cm/s, respectively, after Roseberry *et al.* [2012]). Also note that Figures 4, 6, and 7 all use the same dimensionless form of time.

3.2. Particle Diffusion

The diffusion process quantifies the dispersion of particles as they travel downstream and can be thus described by the growth of the variance of the particle travel distance with time t

$$\sigma_x^2 = \langle (x_t - \langle x \rangle)^2 \rangle \propto t^{\beta_x}. \quad (4)$$

When $\beta_x=1$, particle diffusion is “normal,” i.e., the variance grows linearly with t . When $\beta_x \neq 1$, particle diffusion is “anomalous,” specifically, subdiffusion for $\beta_x < 1$, superdiffusion for $1 < \beta_x < 2$ and ballistic for $\beta_x=2$ [see for e.g., Weeks *et al.*, 1996; Nikora *et al.*, 2002; Martin *et al.*, 2012; Furbish *et al.*, 2012a].

Figure 3b shows that different diffusion regimes are observed for different ranges of investigated time scales. Superdiffusion (more exactly, ballistic) occurs at short time scales due to the inertia of the particles; then, diffusion changes to normal for longer time scales. The two regimes, separated by an approximate threshold time $T_{LI}^0=16$ (corresponding to a dimensional value $T_{LI}=0.4$ s) are consistent with the “local” and “intermediate” scales and with the separating timescale $T_{LI}^0=15$ obtained by Bilal *et al.* [2012].

Although the ratios of \bar{T}_r/\bar{T}_s cover a wide range of scales, the threshold times T_{LI} that separate different diffusion regimes are very similar. Fan *et al.* [2014] obtained that the autocorrelation time scale of the particle velocities series was $\tau_c=0.098$ s under the assumption of transport regime only (if we use episodic motion series, a robust autocorrelation time could not be obtained due to the zero-velocities during resting times). $\tau_c=0.098$ s is however so small that most particles stay within the motion regime [Nikora *et al.*, 2002]. This suggests that, up to $\sim 10^{-1}$ s, particle diffusion is statistically determined through a ballistic process controlled by the initial acceleration of particles entering in the motion regime, and by their inertial properties. The transition timescale emerging from our simulations is of the same order of magnitude, $T_{LI} \sim 4\tau_c$, corresponding, spatially, to a travel distance of ~ 10 particles diameters assuming a particle velocity equal to the shear velocity. The above step length is well within the range of the step length provided in Figure 4, confirming that the transitional time scale statistically marks the transition between the initial transport conditions (within the first step length or hop) and the genuine episodic regime (involving multiple steps and/or alternating step times and resting times).

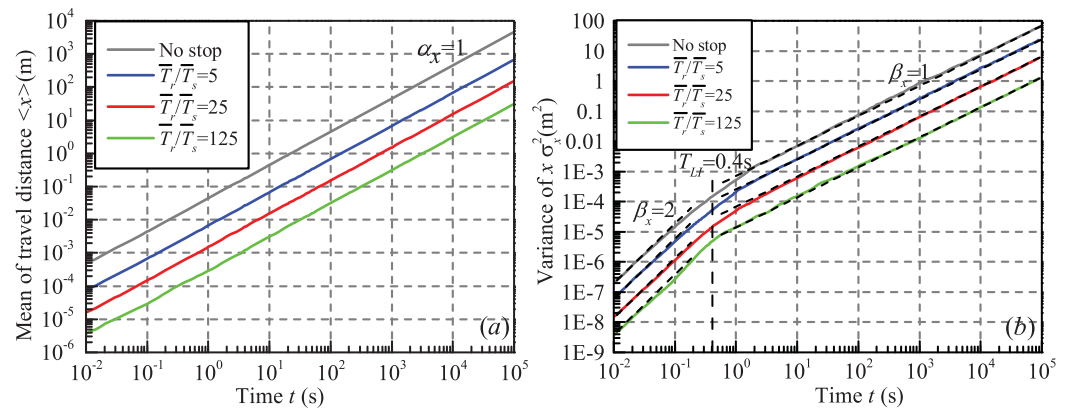


Figure 3. Emergent advection and diffusion regimes as depicted by the mean and variance of travel distance with time. (a) Growth of average travel distance (x) with time for the particles with different mean resting times (note that particles with smaller resting times will transport and disperse faster). Blue, red, and green lines represent diffusion regimes for the ratios of \bar{T}_r/\bar{T}_s equal to 5, 25, and 125, respectively. Advection of particles for no stop ($T_r=0$) is also presented for comparison (gray line). All four conditions mentioned above show normal advection for all studied time scales. (b) Change in diffusion regimes from ballistic to normal. Diffusion of particles for no stop ($T_r=0$) is also presented for comparison (gray line). Thin black-dashed lines indicate the slope of different regimes. The time that separates two regimes $T_{tr}^0=T_{tr}u_*^*/d$ is about 16, which is close to the value 15, obtained by *Bialik et al.* [2012] as the threshold between “local” and “intermediate” diffusions. Also note that x axis represents dimensionless time t normalized by d/u_* , where u_* and d are the friction velocity and particle diameter, respectively.

3.3. Heavy-Tailed Step Lengths Do Not Necessarily Induce Superdiffusion

In section 3.1 and 3.2, both active particle velocities and resting times were thin-tailed resulting in normal advection and diffusion (except for ballistic within very small time scales). However, the distribution of step lengths L_s obtained from our model is heavy-tailed, with a fitted power-law exponent ~ -1.5 , i.e., $f(L_s) \sim L_s^{-1.5}$ (see Figure 4a). The observed normal diffusion from the heavy-tailed step lengths and thin-tailed resting times, obtained from our ELE, does not agree with the random walk model results by *Schumer et al.* [2009] (S-RWM) and *Weeks et al.* [1996] (W-ARWM). We infer that this difference is due to the fact that, in our model, particles achieve the step lengths L_s within finite step times T_s (Figure 5c), while in S-RWM, the step times T_s were considered as zero (Figure 5a). In other words, in S-RWM, the active particle velocity u_p is infinitely large while in our model, the active particle velocity u_p is finite and thin tailed. On the other hand, in the W-ARWM model (Figure 5b), u_p was considered constant in every step. Thus, the normal diffusion regime in our ELE model does not depend on the distribution of the step lengths L_s , but rather on the thin-tailed PDF of the particle velocity u_p . As a limiting condition in our model, if the particles never stop ($\bar{T}_r=0$), the resulting step lengths will be infinitely large, but the diffusion regime will still be normal (see Figure 3b, gray line).

4. ELE With Power-Law PDF of Resting Times

In this section, we use a different distribution of resting times T_r : a common power-law PDF named Pareto distribution, given as

$$f(T_r) = (\nu - 1)a^{\nu-1}T_r^{-\nu} \quad (5)$$

where ν is the tail index, and a is the minimum possible value above which the distribution is defined ($T_r \geq a$). Among the several values of the ν parameter investigated (not all shown for brevity), here we selected two for which the transport model exhibits superdiffusion ($\nu=1.6$) and subdiffusion ($\nu=1.4$). In order to compare travel distance statistics for exponential and power-law distributions of the resting times, for a given value of ν , we define different values of a to ensure that the diffusion characteristics are comparable, at least for a range of timescales (see Figures 3b and 7b). This is achieved for $a=1/5000$ and $1/50$, for $\nu=1.4$ and 1.6 , respectively. The PDFs of the exponential and power-law resting times are presented for comparison in Figure 6. As expected, the PDFs of power-law distributed resting times decay much slower than the exponential distributed resting times.

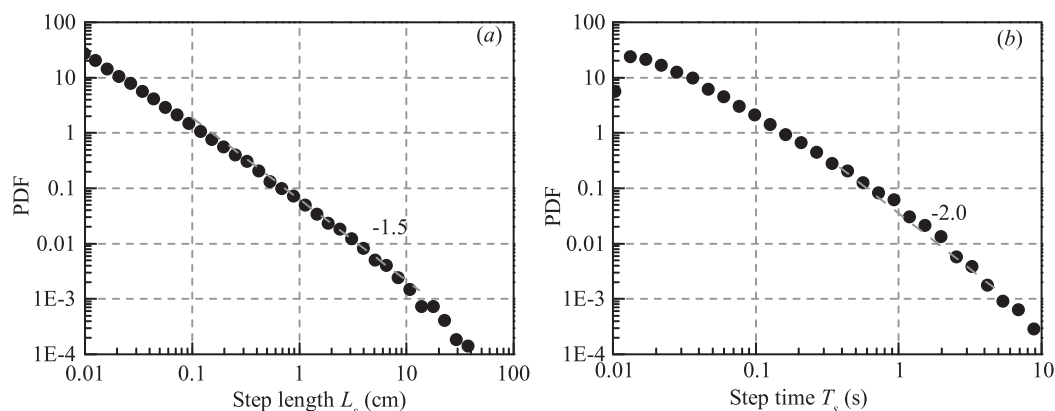


Figure 4. PDFs of simulated particles (a) for step lengths and (b) for step times. Both PDFs show power-law tails with exponents ~ -1.5 and ~ -2.0 for step lengths and step times, respectively.

4.1. Particle Advection

Figure 7a describes the particle advection regimes for two power-law resting time distributions, with $\nu=1.4$ and $\nu=1.6$, respectively, and compared to an exponential resting time distribution (here with the ratio $\bar{T}_r/\bar{T}_s=25$). For both power-law distributed T_r , at small time scales, normal advection ($\alpha_x=1$) is observed, though progressively reduced exponents ($\alpha_x < 1$) at large time scales lead to subadvection with $\alpha_x=0.6$ and 0.4 , respectively. Our simulations show that in the range $1 < \nu < 2$, subadvection emerges at large time scales, consistent with the model by Schumer *et al.* [2009] for thin-tailed steps L_s , and different resting time distributions. Note that, subadvection means that the average travel distance grows slower than linear with time, which leads to a temporal decrease of the average virtual particle velocity \bar{U}_{vx} . This phenomenon was also observed in natural rivers for bed load transport, see Ferguson and Hoey [2002].

4.2. Particle Diffusion

Figure 7b shows the different diffusion regimes for the same resting time distributions tested above. At small time scales, both power-law distributed T_r ($\nu=1.4$ and 1.6) lead to a ballistic diffusion regime, while at larger time scales, the diffusion changes from superdiffusion ($\beta_x=1.2$ for $\nu=1.6$) to subdiffusion ($\beta_x=0.8$ for $\nu=1.4$). Note that both anomalous diffusion and anomalous advection occur at nearly the same time scale (compare Figures 7a and 7b). Also note that, for $\nu=1.4$, at very small time scales over ballistic diffusion regime emerges, which may be due to the fact that the group of particles in motion has not reached a steady state at those small time scales [see Fan 2014; Campagnol *et al.*, 2015].

Contrary to the general understanding that power-law distribution of resting time would result in subdiffusion [e.g., Nikora *et al.*, 2002; Schumer *et al.*, 2009], our simulations show that both superdiffusion and subdiffusion could occur as a result of different tail parameters ν of the power-law T_r distribution. An extended discussion about this observation is presented in section 6.

4.3. Transition Times From Normal to Anomalous Advection and Diffusion Regimes: Sensitivity Analysis

In this section, we perform sensitivity analysis to study how the transition times from normal to anomalous advection/diffusion (T_{NA}) are affected by the model parameters. For this, first, we keep the same rest state model and change the motion state model by changing the shear velocity u_* to twice and four times (the corresponding diffusion parameter D_x is also increased by twice and four times, see Fan *et al.* [2014]). However, the observed transition time from normal to anomalous advection/diffusion regimes does not change, for e.g., $T_{NA} = 2000$ s for three cases. Second, we keep the same motion state model and change the rest state model by changing a (which reflects the magnitude of the heavy tailed variables) to twice and four times, even though the mean value may not converge. The results reveal that a larger magnitude of rest times induces longer transition times from normal to anomalous advection/diffusion regimes ($T_{NA} = 2000, 4000, \text{ and } 8000$ s, for given a value, twice, and four times a , respectively). Specifically, when comparing the advection and diffusion regimes under the same combination of motion and rest models, the transition times T_{NA} , from normal to anomalous advection, are always the same as those from normal to anomalous

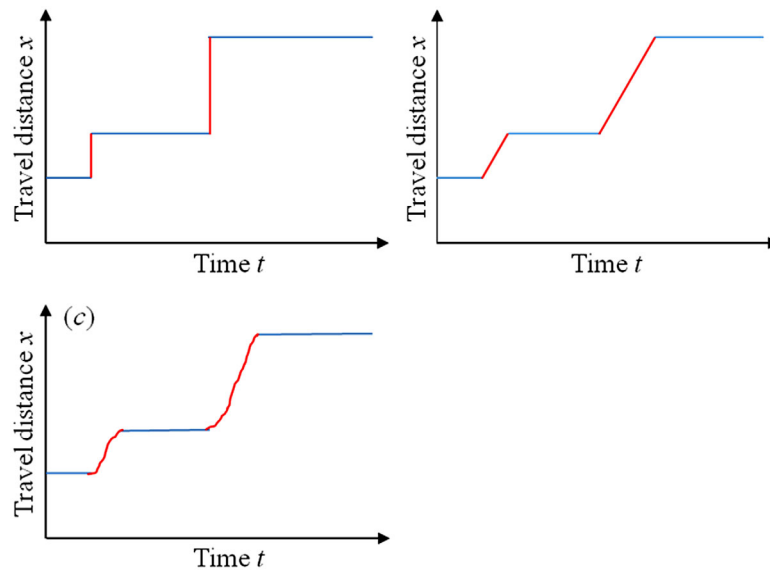


Figure 5. Definition sketches of different models. (a) Model by *Schumer et al.* [2009] (S-RWM), the steps are achieved instantaneously; (b) Model by *Weeks et al.* [1996] (W-ARWM), the steps are achieved within a finite time, and all the velocities during the steps are kept constant; and (c) Semimechanistic ELE model from this study, the steps are achieved with finite time and the velocities are stochastic.

diffusion. In summary, T_{NA} does not depend on the motion regime, but depends on the rest regime; mostly on the thin/thick tails of the PDF of the resting times, and only marginally on the mean resting times for exponential PDF.

5. Advection and Diffusion Regimes From an Episodic Framework Using the Langevin Equation by *Ancey and Heyman* [2014]

The Langevin equation (LE) by *Fan et al.* [2014] was developed for low transport rate conditions (particles are rolling and/or sliding on the bed). For high transport rate conditions (saltating particles), *Ancey and Heyman* [2014] developed a Langevin equation calibrated using their own experimental data. Here we incorporate the Langevin equation by *Ancey and Heyman* [2014] into our episodic framework to simulate the episodic motion regime of particles. For simulation purposes, we used their own parameters as $\bar{u}_p = 0.299$

$m \cdot s^{-1}$ and $\bar{u}_p / \sqrt{D/t_r} = 5.7$ calibrated from their experiments. Note that the value of D and t_r were not provided independently in *Ancey and Heyman* [2014]; as a result, we estimated the independent particle relaxation time t_r as the ratio between the settling velocity (computed as in *Cheng* [1997]) and the acceleration due to gravity [*Zhong et al.*, 2011]. The computed values of t_r and D are 0.0332 s and $9.13 \times 10^{-5} m^2 \cdot s^{-1}$, respectively. For more details about the model formulation, see *Ancey and Heyman* [2014].

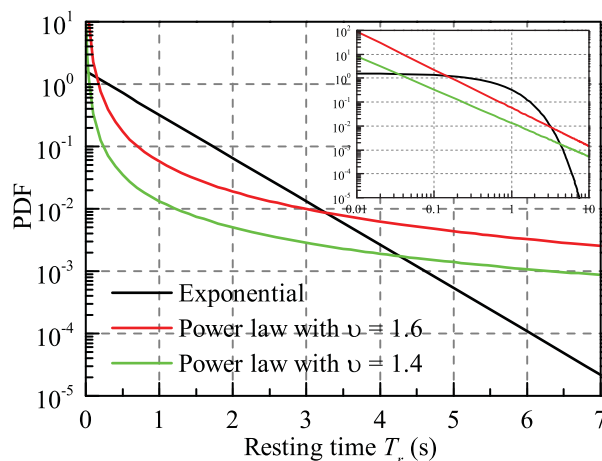


Figure 6. PDFs of resting times used in the Episodic Langevin Equation (ELE) model. Black, red and green lines represent exponential distribution with average 0.625 s, power law with $\nu = 1.6, a = 1/50$ and power law with $\nu = 1.4, a = 1/5000$, respectively. The inset shows the same distributions on log-log scale for comparison.

We further imposed the particle velocity to be zero when its velocity turns to negative, forcing the particle to stop (the velocity remains zero) for a duration defined by the stochastic resting time T_r (particle resting regime), according to our ELE framework. For incorporating resting time in the model,

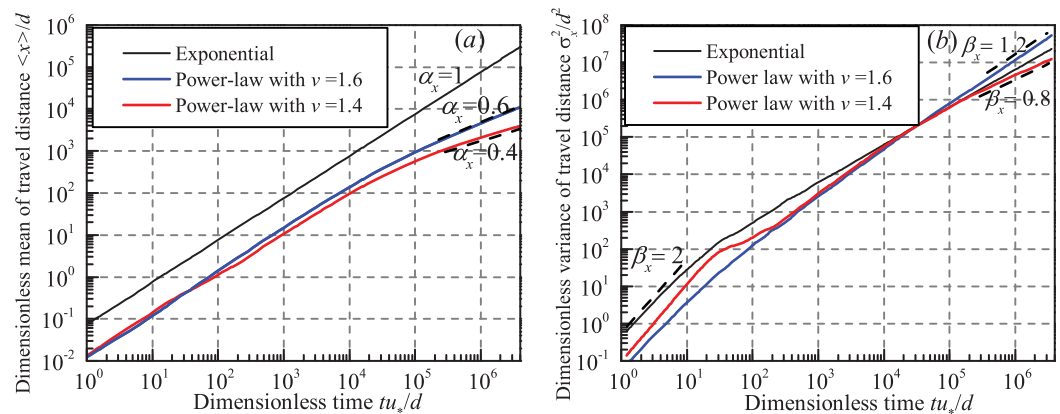


Figure 7. Power-law resting times leading to anomalous transport. (a) advection (growth of mean travel distance $\langle x \rangle$ with time). For particles with heavy tailed resting time with $\nu=1.6$ (blue line) and $\nu=1.4$ (red line), the mean travel distance grows slower than linearly, with $\alpha_x=0.6$ and $\alpha_x=0.4$, which show subadvection. Linear growth of $\langle x \rangle$ with time for particles with exponential resting time ($\bar{T}_r/\bar{T}_s=25$, black line) is also presented for comparison. (b) Diffusion (variance of travel distance with time); diffusion at large time scales and the normal diffusion with exponential resting times are also presented for comparison. Resting times with $\nu=1.6$ show superdiffusion while resting times with $\nu=1.4$ show subdiffusion. Only very heavy-tailed resting times ($\nu < 1.5$) lead to subdiffusion and for larger scales the regimes are characterized by $\beta_x=2\nu-2$. Note that x axis represents dimensionless time t normalized by d/u_s , where u_s and d are the friction velocity and particle diameter, respectively.

we used exponential and heavy-tailed distributed resting times. For comparison purposes, we used $\bar{T}_r=0.625$ s for the exponentially distributed resting times T_r , (derived imposing $\bar{T}_r/\bar{T}_s=25$ and $\bar{T}_s=0.05$ s, consistent with our ELE parameters). Similarly, for the heavy-tailed distributed resting times T_r , we chose $\nu=1.4$ and 1.6 , respectively.

Although the time scales of advection and diffusion regimes obtained from the episodic *Ancey and Heyman* [2014] model (Figure 8) are larger than those in our ELE (Figure 7), as a result of the different \bar{T}_r/\bar{T}_s ratio, similar emergent advection and diffusion regimes are observed. Recall that active particle velocities from both LE by *Fan et al.* [2014] and *Ancey and Heyman* [2014] are thin-tailed (exponential and Gaussian, respectively), suggesting that the emergent advection and diffusion regimes are only determined by the PDF of the resting times, as far as the PDF of active particle velocities remains thin tailed.

In addition, we must recognize that both the *Fan et al.* [2014] and *Ancey and Heyman* [2014] models are calibrated using experimental observations. So any effect of particle collisions on the distribution of particle velocity, would be accounted for indirectly in the model parameters. That said, we acknowledge that our model however does not treat particle collisions in a mechanistic way. Hence, applying our model, or the

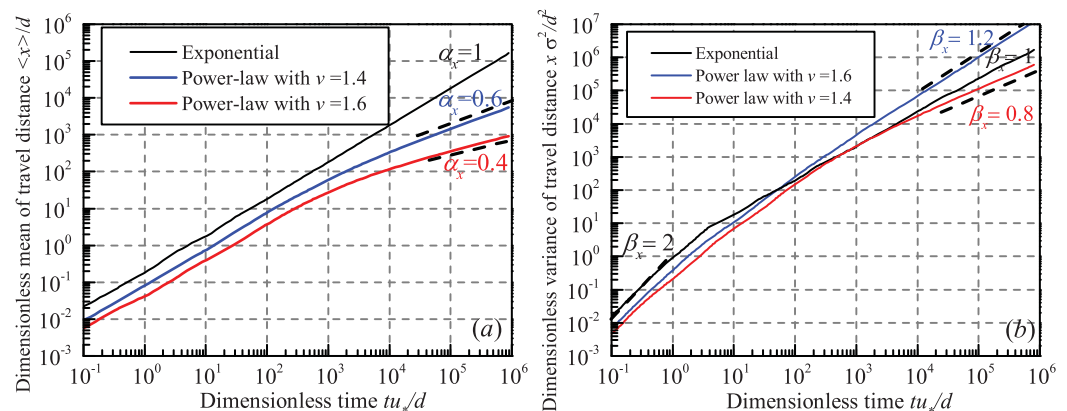


Figure 8. Normal and anomalous transport obtained by incorporating an episodic framework in the Langevin equation of *Ancey and Heyman* [2014]. (a) The emergent advection and (b) diffusion regimes are the same as those obtained from our Episodic Langevin Equation (ELE) model (see Figure 7 for comparison). Note that x axis represents dimensionless time t normalized by d/u_s , where u_s and d are the friction velocity and particle diameter, respectively.

Table 1. Advection and Diffusion Regimes at Large Time Scales Obtained From the Three Different Models^a

Models	Conditions of ν	Advection Exponent α_x	Diffusion Exponent β_x
<i>Schumer et al.</i> [2009]	$1 < \nu < 2$	$\nu - 1$	$\nu - 1$
	$\nu > 2$	1	1
<i>Weeks et al.</i> [1996]	$1 < \nu < 2$	$\nu - 1$	$2\nu - 2$
	$2 < \nu < 3$	1	$4 - \nu$
	$\nu > 3$	1	1
This study	$1 < \nu < 2$	$\nu - 1$	$2\nu - 2$
	$2 < \nu < 3$	1	$4 - \nu$
	$\nu > 3$	1	1

^aThe random walk model by *Schumer et al.* [2009] (S-RWM), the asymmetric random walk model by *Weeks et al.* [1996] (W-ARWM), and the semimechanistic Episodic Langevin Equation (ELE) model from the current study.

(W-ARWM) used random walk models to study the episodic motion of particles with different distributions of step lengths $f(L_s) \sim L_s^{-\mu}$ and resting times $f(T_r) \sim T_r^{-\nu}$, and explored the corresponding advection and diffusion regimes associated with the different tail parameters μ and ν . Figures 5a and 5b show the schematic of S-RWM, W-ARWM for comparison purposes. As discussed above, in S-RWM (Figure 5a), steps were achieved instantaneously, and thus active particle velocities were infinitely large. In W-ARWM (Figure 5b), the steps were assumed to be resolved within a finite time, with constant velocities during particle motion. In our ELE model (Figure 5c), the steps are also occurring within a finite time, but the associated particle velocities are stochastic, which represents an increased degree of complexity with respect to the approach of *Weeks et al.* [1996] and, in our opinion, a model improvement.

Table 1 shows the advection and diffusion characteristics resulting from a range of values of the resting time tail parameter ν , using the three models under investigation S-RWM, W-ARWM, and our ELE. Note that in the two models S-RWM and W-ARWM, we impose the step lengths L_s to be thin tailed.

6.2. Coupled and Uncoupled Step Times With Associated Step Lengths

In this section, we further investigate the fundamental differences between the three approaches (S-RWM, W-ARWM, and our ELE), specifically, whether the step times and the associated step lengths in these models are coupled or not. As discussed above, in S-RWM, the step times were assumed to be zero, and thus the step lengths are not correlated to the step times, while in W-ARWM and in our ELE models the step times and the associated step lengths are related as $L_s \propto T_s$ and $L_s \propto T_s^{1.6}$, respectively (see Figure 2b for ELE), and thus coupled. The correlation between step lengths and step times explains the different diffusion regimes as seen in our ELE and W-ARWM compared to S-RWM. Moreover, if the step lengths and step times are correlated, the fractional advection-diffusion equation as in *Schumer et al.* [2009] cannot be used, as suggested by *Pelosi et al.*, [2014]. However, if the step times T_s are nonzero, and the step lengths L_s have no relationship with the step times T_s , the spatial and temporal statistical characteristics are uncoupled, and thus the S-RWM and the fractional advection-diffusion equation could still be used.

From the above discussion, we notice that for the advection characteristics (first-order moment of travel distance x), all three models (ELE, with motion regimes modeled following *Fan et al.* [2014] or *Ancey and Heyman* [2014], S-RWM, and W-ARWM) reproduce the same advection regime, whereas only the W-ARWM and ELE models reproduce the same diffusion regime. We suggest that S-RWM is too simplified for the study of diffusion of bed load particles, though it is still appropriate for the study of anomalous deposition rate [*Schumer and Jerolmack*, 2009] and incision rate of bed rock rivers [*Stark et al.*, 2009; *Finnegan et al.*, 2014], which depend on the first-order moment of the stochastic variables. Based on this, we suggest that progressively higher-order moments of travel distances (in general, modeled stochastic variables) might be required to differentiate between competing models of resting and motion regimes.

7. Summary and Conclusions

In this paper, we built an episodic semimechanistic framework to simulate the transport of uniform tracer particles, with steps separated by rests, and studied the emergent (normal or anomalous) particle advection-diffusion regimes. In our framework, states of motion and rest were modeled independently,

Ancey and Heyman [2014] model, to higher transport conditions can be done only if the transport parameters are recalibrated on the resulting particle velocity distribution.

6. Discussion

6.1. Comparison of ELE With Different Random Walk Models

Both *Schumer et al.* [2009] (S-RWM) and *Weeks et al.* [1996]

with two different models for the particle motion state [Fan et al. 2014; Ancey and Heyman, 2014] incorporated and tested. We explored how different resting time distributions affect particle advection and diffusion, under the constraint of thin tailed velocities [Fan et al. 2014; Furbish et al. 2012b; Ancey and Heyman, 2014].

For exponentially distributed resting times T_r , thin-tailed active particle velocities u_p were observed to play a dominant role in the diffusion regime: at longer time scales, diffusion was observed to be normal instead of superdiffusive, even if the step lengths were heavy tailed. Instead, assuming a power-law distribution of the resting times with a tail parameter ν , led to four different regimes identified based on the resulting particle advection and diffusion parameters: (I) $1 < \nu < 1.5$, sub-advection and subdiffusion; (II) $1.5 < \nu < 2$, subadvection and super-diffusion; (III) $2 < \nu < 3$, normal-advection and superdiffusion; and (IV) $\nu > 3$ normal-advection and normal-diffusion.

Our results also suggest that the assumption of instantaneous steps L_s , used e.g., in Schumer et al. [2009], could only reproduce the same advection regime, but results in a different diffusion regime as compared to our more complex semimechanistic model or to the Weeks et al. [1996] model (with finite step times).

We acknowledge, as a major limitation of our approach, the fact that the model governing particle motion is totally independent from the resting time model: while the first one has been calibrated in two monitored transport conditions using the Roseberry et al. [2012] and Ancey and Heyman [2014] data, the second one could not be verified, in any known conditions, due to the lack of experimental measurements. As a result, we elaborated how different resting time models influence particle advection and diffusion regimes at different time scales. Further observations of resting times would be needed to assess the predictive capabilities of the proposed model and its utility as a diagnostic tool for guiding hypotheses of sediment transport regimes in real rivers.

Notation

a	minimum possible value for Pareto distribution.
D_x	the amplitude of fluctuation force in the streamwise direction [$L^3 \cdot T^{-2}$].
d	diameter of the particle [L].
D	equivalent of a particle diffusivity [$L^2 \cdot T^{-1}$].
D_x	mean downstream force exerted on a particle of unit mass [$L \cdot T^{-2}$].
F_1, F_2	Runge-Kutta coefficients.
g	gravity acceleration [$L \cdot T^{-2}$].
L_s	step length [L].
t	time [T].
t_r	particle relaxation time [T].
T_{LI}	The threshold of local and intermediate time scales for particle diffusion [T].
T_s	step time [T].
T_r	resting time [T].
u_p	streamwise particle velocity [$L \cdot T^{-1}$].
\bar{u}_p	mean streamwise velocity of particles [$L \cdot T^{-1}$].
u_*	bed friction velocity [$L \cdot T^{-1}$].
U_{vx}	virtual velocity for the particles moving episodically [$L \cdot T^{-1}$].
w_0	w_1, w_2 three independent standard Gaussian distribution random numbers.
x	travel distance in streamwise direction [L].
α_x	the exponent for advection, namely, the power-law exponent for mean of travel distance x with time.
β_x	the exponent for diffusion, namely, the power-law exponent for variance of travel distance x with time.
δ	delta function.
Δ_x	friction force in streamwise direction [$L \cdot T^{-2}$].
μ, ν	the tail parameter for power-law step length L_s and resting time T_r , respectively.
ξ_x	Gaussian white noise force in streamwise direction [$L \cdot T^{-2}$].
τ_c	autocorrelation time of particle velocities time series [T].

Acknowledgments

The authors are thankful to Vamsi Ganti and Rina Schumer for insightful discussions. We thank the editor Graham Sander, the associate editor Christophe Ancey, Francesco Ballio, and three anonymous reviewers for their constructive comments. Financial support from National Natural Science Foundation of China (51509172, 51539007), Science Project of China (2012BAB05B02), Sichuan University (2015SCU11046), and support from the U.S. National Science Foundation (NSF) under a Water Sustainability and Climate project (grant CBET-1209402), as well as an International Research project (LIFE: NSF grant EAR-1242458) are gratefully acknowledged. The first author received a fellowship from the China Scholarship Council. All the simulated data in this paper can be requested from the authors.

References

- Ancey, C. (2010), Stochastic modeling in sediment dynamics: Exner equation for planar bed incipient bed load transport conditions, *J. Geophys. Res.*, *115*, F00A11, doi:10.1029/2009JF001260.
- Ancey, C., and J. Heyman (2014), A microstructural approach to bed load transport: Mean behaviour and fluctuations of particle transport rates, *J. Fluid Mech.*, *744*, 129–168.
- Ancey, C., T. Böhm, M. Jodeau, and P. Frey (2006), Statistical description of sediment transport experiments, *Phys. Rev. E*, *74*, 011302, doi:10.1103/PhysRevE.74.011302.
- Ballio, F., J. Campagnol, V. Nikora and A. Radice (2013), Diffusive properties of bed load moving sediments at short time scales [CD], in *Proceeding of 2013 IAHR World Conference*, Chengdu, China.
- Bialik, R. J., V. I. Nikora, and P. M. Rowinski (2012), 3D Lagrangian modelling of saltating particles diffusion in turbulent water flow, *Acta Geophys.*, *60*(6), 1639–1660.
- Bradley, D. N., G. E. Tucker, and D. A. Benson (2010), Fractional dispersion in a sand bed river, *J. Geophys. Res.*, *115*, F00A09, doi:10.1029/2009JF001268.
- Campagnol J., A. Radice, F. Ballio, and V. Nikora (2015), Particle motion and diffusion at weak bed load: Accounting for unsteadiness effects of entrainment and disentrainment, *J. Hydraul. Res.*, *53*(5), 633–648.
- Cheng, N. S. (1997), Simplified settling velocity formula for sediment particle, *J. Hydraul.*, *123*(2), 149–152.
- Cristo, C., M. Greco, M. Iervolino, A. Leopardi, and A. Vacca (2015) Two-dimensional two-phase depth-integrated model for transients over mobile bed, *J. Hydraul. Eng.*, *142*(2), 1–20, doi:10.1061/(ASCE)HY.1943-7900.0001024, 04015043.
- Drake, T. G., R. L. Shreve, W. E. Dietrich, P. J. Whiting, and L. B. Leopold (1988), Bedload transport of fine gravel observed by motion-picture photography, *J. Fluid Mech.*, *192*, 193–217.
- Einstein, H. A. (1937), Der Geschiebetrieb als Wahrscheinlichkeitsproblem, in *Mitteilung der Versuchsanstalt für Wasserbau an der Eidgenössische Technische Hochschule Zürich*, Rascher, Zurich, Switzerland [English translation, Sedimentation], edited by H. W. Shen, pp. C1–C105, Colo. State Univ., Fort Collins.
- Fan, N. (2014), Bed load transport: From individual particle forces to group transport behavior [in Chinese], PhD thesis, Tsinghua Univ., Beijing, China.
- Fan, N., D. Zhong, B. Wu, E. Foufoula-Georgiou, and M. Guala (2014), A mechanistic-stochastic formulation of bed load particle motions: From individual particle forces to the Fokker-Planck equation under low transport rates, *J. Geophys. Res. Earth Surf.*, *119*, 464–482, doi:10.1002/2013JF002823.
- Fathel, S. L., D. J. Furbish, and M. W. Schmeeckle (2015), Experimental evidence of statistical ensemble behavior in bed load sediment transport, *J. Geophys. Res. Earth Surf.*, *120*, 2298–2317, doi:10.1002/2015JF003552.
- Ferguson, R. I., and T. B. Hoey (2002), Long-term slowdown of river tracer pebbles: Generic models and implications for interpreting short-term tracer studies, *Water Resour. Res.*, *38*(8), 1142, doi:10.1029/2001WR000637.
- Ferguson, R. I., and S. J. Wathen (1998), Tracer-pebble movement along a concave river profile: Virtual velocity in relation to grain size and shear stress, *Water Resour. Res.*, *34*(8), 2031–2038.
- Finnegan, N. J., R. Schumer, and S. Finnegan (2014), A signature of transience in bedrock river incision rates over timescales of 10(4)–10(7) years, *Nature*, *505*(7483), 391–394.
- Furbish, D. J., and M. W. Schmeeckle (2013), A probabilistic derivation of the exponential-like distribution of bed load particle velocities, *Water Resour. Res.*, *49*, 1537–1551, doi:10.1002/wrcr.20074.
- Furbish, D. J., A. E. Ball, and M. W. Schmeeckle (2012a), A probabilistic description of the bed load sediment flux: 4. Fickian diffusion at low transport rates, *J. Geophys. Res.*, *117*, F03034, doi:10.1029/2012JF002356.
- Furbish, D. J., P. K. Haff, J. C. Roseberry, and M. W. Schmeeckle (2012b), A probabilistic description of the bed load sediment flux: 1. Theory, *J. Geophys. Res.*, *117*, F03031, doi:10.1029/2012JF002352.
- Furbish, D. J., J. C. Roseberry, and M. W. Schmeeckle (2012c), A probabilistic description of the bed load sediment flux: 3. The particle velocity distribution and the diffusive flux, *J. Geophys. Res.*, *117*, F03033, doi:10.1029/2012JF002355.
- Ganti, V., M. M. Meerschaert, E. Foufoula-Georgiou, E. Viparelli, and G. Parker (2010), Normal and anomalous diffusion of gravel tracer particles in rivers, *J. Geophys. Res.*, *115*, F00A12, doi:10.1029/2008JF001222.
- Guala, M., A. Singh, N. BadHeartBull, and E. Foufoula-Georgiou (2014), Spectral description of migrating bedforms and sediment transport, *J. Geophys. Res. Earth Surf.*, *119*, 123–137, doi:10.1002/2013JF002759.
- Habersack, H. M. (2001), Radio-tracking gravel particles in a large braided river in New Zealand: A field test of the stochastic theory of bed load transport proposed by Einstein, *Hydrol. Processes*, *15*(3), 377–391.
- Han, Q. W., and M. M. He (1980), Stochastic models for bed load particle diffusion and the statistical properties [in Chinese], *Sci. China*, *4*, 396–401.
- Haschenburger, J. K. (2013), Tracing river gravels: Insights into dispersion from a long-term field experiment, *Geomorphology*, *200*(S1), 121–131.
- Hassan, M. A., M. Church, and A. P. Schick (1991), Distance of movement of coarse particles in gravel bed streams, *Water Resour. Res.*, *27*(4), 503–511.
- Hassan, M. A., H. Voepel, R. Schumer, G. Parker, and L. Fraccarollo (2013), Displacement characteristics of coarse fluvial bed sediment, *J. Geophys. Res. Solid Earth*, *118*, 155–165, doi:10.1029/2012JF002374.
- Hill, K. M., L. Dell'Angelo, and M. M. Meerschaert (2010), Heavy-tailed travel distance in gravel bed transport: An exploratory enquiry, *J. Geophys. Res.*, *115*, F00A14, doi:10.1029/2009JF001276.
- Julien, P. and B. Bounvilay (2013), Velocity of rolling bed load particles, *J. Hydraul. Eng.*, *139*(2), 177–186, doi:10.1061/(ASCE)HY.1943-7900.0000657.
- Keylock, C. J., A. Singh, and E. Foufoula-Georgiou (2014), The complexity of gravel bed river topography examined with gradual wavelet reconstruction, *J. Geophys. Res. Earth Surf.*, *119*, 682–700, doi:10.1002/2013JF002999.
- Lajeunesse, E., L. Malverti, and F. Charru (2010), Bed load transport in turbulent flow at the grain scale: Experiments and modeling, *J. Geophys. Res.*, *115*, F04001, doi:10.1029/2009JF001628.
- Martin, R. L., D. J. Jerolmack, and R. Schumer (2012), The physical basis for anomalous diffusion in bed load transport, *J. Geophys. Res.*, *117*, F01018, doi:10.1029/2011JF002075.
- Martin, R. L., P. K. Purohit, and D. J. Jerolmack (2014), Sedimentary bed evolution as a mean-reverting random walk: Implications for tracer statistics, *Geophys. Res. Lett.*, *41*, 6152–6159, doi:10.1002/2014GL060525.
- McElroy, B., and D. Mohrig (2012), Nature of deformation of sandy bed forms, *J. Geophys. Res.*, *117*, F04025, doi:10.1029/2012JF002642.

- Nikora, V., J. Heald, D. Goring, and I. McEwan (2001), Diffusion of saltating particles in unidirectional water flow over a rough granular bed, *J. Phys. A. Math. Gen.*, *34*(50), L743–L749.
- Nikora, V., H. Habersack, T. Huber, and I. McEwan (2002), On bed particle diffusion in gravel bed flows under weak bed load transport, *Water Resour. Res.*, *38*, 1081, doi:10.1029/2001WR000513.
- Papanicolaou, A. N., P. Diplas, M. Balakrishnan, and C. L. Dancy (1999), Computer vision technique for tracking bed load movement, *J. Comput. Civ. Eng.*, *13*(2), 71–79.
- Pelosi, A., G. Parker, R. Schumer and H. B. Ma (2014), Exner-Based Master Equation for transport and dispersion of river pebble tracers: Derivation, asymptotic forms, and quantification of nonlocal vertical dispersion, *J. Geophys. Res. Earth Surf.*, *119*, 1818–1832, doi:10.1002/2014JF003130.
- Phillips, C. B., R. L. Martin, and D. J. Jerolmack (2013), Impulse framework for unsteady flows reveals superdiffusive bed load transport, *Geophys. Res. Lett.*, *40*, 1328–1333, doi:10.1002/grl.50323.
- Ramesh, B., U. C. Kothiyari, and K. Murugesan (2011), Near-bed particle motion over transitionally-rough bed, *J. Hydraul. Res.*, *49*(6), 757–765, doi:10.1080/00221686.2011.620369.
- Roseberry, J. C., M. W. Schmeeckle, and D. J. Furbish (2012), A probabilistic description of the bed load sediment flux: 2. Particle activity and motions, *J. Geophys. Res.*, *117*, F03032, doi:10.1029/2012JF002353.
- Sayre, W., and D. Hubbell (1965), Transport and dispersion of labeled bed material, North Loup River, Nebraska, *U.S. Geol. Surv. Prof. Pap.*, *433-C*, 48 pp.
- Schmidt, K. H., and P. Ergenzinger (1992), Bedload entrainment, travel lengths, step lengths, rest periods - studied with passive (iron, magnetic) and active (radio) tracer techniques, *Earth Surf. Processes Landforms*, *17*(2), 147–165.
- Schumer, R., and D. Jerolmack (2009), Real and apparent changes in sediment deposition rates through time, *J. Geophys. Res.*, *114*, F00A06, doi:10.1002/esp.3290170204.
- Schumer, R., M. M. Meerschaert, and B. Baeumer (2009), Fractional advection-dispersion equations for modeling transport at the Earth surface, *J. Geophys. Res.*, *114*, F00A07, doi:10.1029/2008JF001246.
- Sekine, M., and G. Parker (1992), Bed-load transport on transverse slope.1, *J. Hydraul. Eng.*, *118*(4), 513–535.
- Singh, A., K. Fienberg, D. J. Jerolmack, J. Marr, and E. Foufoula-Georgiou (2009), Experimental evidence for statistical scaling and intermittency in sediment transport rates, *J. Geophys. Res.*, *114*, F01025, doi:10.1029/2007JF000963.
- Singh, A., S. Lanzoni, P. R. Wilcock, and E. Foufoula-Georgiou (2011), Multiscale statistical characterization of migrating bed forms in gravel and sand bed rivers, *Water Resour. Res.*, *47*, W12526, doi:10.1029/2010WR010122.
- Singh, A., E. Foufoula-Georgiou, F. Porte-Agel, and P. R. Wilcock (2012), Coupled dynamics of the co-evolution of gravel bed topography, flow turbulence and sediment transport in an experimental channel, *J. Geophys. Res.*, *117*, F04016, doi:10.1029/2011JF002323.
- Stark, C. P., E. Foufoula-Georgiou, and V. Ganti (2009), A nonlocal theory of sediment buffering and bedrock channel evolution, *J. Geophys. Res.*, *114*, F01029, doi:10.1029/2008JF000981.
- Todorovic, P. (1982), A stochastic model of longitudinal dispersion of bed sediment based on the granulation function, *Adv. Water Resour.*, *5*(1), 42–46.
- Valyrakis, M., P. Diplas, and C. L. Dancy (2011), Entrainment of coarse grains in turbulent flows: An extreme value theory approach, *Water Resour. Res.*, *47*, W09512, doi:10.1029/2010WR010236.
- Voepel, H., R. Schumer, and M. A. Hassan (2013), Sediment residence time distributions: Theory and application from bed elevation measurements, *J. Geophys. Res. Earth Surf.*, *118*, 2557–2567, doi:10.1002/jgrf.20151.
- Weeks, E. R., and H. L. Swinney (1998), Anomalous diffusion resulting from strongly asymmetric random walks, *Phys. Rev. E*, *57*(5A), 4915–4920.
- Weeks, E. R., J. S. Urbach, and H. L. Swinney (1996), Anomalous diffusion in asymmetric random walks with a quasi-geostrophic flow example, *Physica D*, *97*(1–3), 291–310.
- Wu, F. C., and K. H. Yang (2004), A stochastic partial transport model for mixed-size sediment: Application to assessment of fractional mobility, *Water Resour. Res.*, *40*, W045014, doi:10.1029/2003WR002256.
- Yang, C. T., and W. W. Sayre (1971), Stochastic model for sand dispersion, *J. Hydraul. Div. Am. Soc. Civ. Eng.*, *97*, 265–288.
- Zhang, Y., M. M. Meerschaert, and A. I. Packman (2012), Linking fluvial bed sediment transport across scales, *Geophys. Res. Lett.*, *39*, L20404, doi:10.1029/2012GL053476.
- Zhang, Y., R. L. Martin, D. Chen, B. Baeumer, H. Sun and L. Chen (2014), A subordinated advection model for uniform bed load transport from local to regional scales, *J. Geophys. Res. Earth Surf.*, *119*, 2711–2729.
- Zhong, D. Y., G. Q. Wang, and Q. C. Sun (2011), Transport equation for suspended sediment based on two-fluid model of solid/liquid two-phase flows, *J. Hydraul. Eng.*, *137*(5), 530–542, doi:10.1061/(ASCE)HY.1943-7900.0000331.